Utilization of pumpkin (*Cucurbita pepo*) seed husks as a low-cost sorbent for removing anionic and cationic dyes from aqueous solutions

Agata Kowalkowska, Tomasz Jóźwiak*

Department of Environmental Engineering, University of Warmia and Mazury in Olsztyn, ul. Warszawska 117a, 10-957 Olsztyn, Poland, emails: tomasz.jozwiak@uwm.edu.pl (T. Jóźwiak), agata.kowalkowska19@wp.pl (A. Kowalkowska)

ABSTRACT

The aim of this study was to examine the possibility of using pumpkin (*Cucurbita pepo*) seed husks as a low-cost sorbent to remove dyes popular in the textile industry, that is, anionic dyes: Reactive Black 5 (RB5) and Reactive Yellow 84 (RY84), and cationic dyes: Basic Violet 10 (BV10) and Basic Red 46 (BR46). The sorbent was subjected to the Fourier-transform infrared spectroscopy (FTIR) analysis. The scope of the research included also the determination of pH (pH 2–11) influence on the efficiency of dye sorption, sorption kinetics (equilibrium time, pseudo-first-order model, pseudo-second-order model, intramolecular diffusion model), and sorption capacity (Langmuir 1 and 2 models, Freundlich model). The optimum pH range for RB5 and RY84 sorption on the tested sorbent was pH 2–3. In the case of BV10, sorption was most effective at pH 3 and in the case of BR46 at pH 6. In each case, the best fit to the experimental data was shown for the pseudo-second order model. The intramolecular diffusion model showed the sorption of each dye to proceed in the three main stages, varying in intensity and duration. Pumpkin seed husk sorption capacity of the anionic dyes was 0.96 mg g^{-1} for RB5 and 1.08 mg g^{-1} for RY84. In the case of cationic dyes, the sorption capacities of the tested sorbent were many time higher and reached 96.01 mg g^{-1} for BV10 and 163.39 mg g^{-1} for BR46.

Keywords: Sorption; Unconventional sorbents; Pumpkin seed husk; Dyes

1. Introduction

Approximately 1 million tons of dyes are produced annually for the needs of the textile, tanning, paper, and food industries. Depending on the type of materials to be dyed and the dyeing technology used, from 10% to 50% of the dye used in the process remain in the post-production wastewater [1]. Dyes discharged to the aquatic environment with untreated wastewater can cause a number of adverse changes in the ecosystem. Even their low concentrations have negative effects on the appearance of water reservoirs [2]. A serious problem is posed by the fact that they restrict plants' access to sunlight, which results in a diminished photosynthesis efficiency. In addition, they suppress oxygen diffusion in water, which - when coupled with poor photosynthesis -

may lead to oxygen deficits in the water environment [3]. Noteworthy are also the toxic and even mutagenic effects of some dyes and products of their partial decomposition on the aquatic organisms. As a consequence, dyes may lead to the reduction of biodiversity in natural water reservoirs and even to the degradation of aquatic ecosystems [4].

Considering the perspective of environment degradation by industrial dyes, it seems advisable to apply effective and environmentally friendly methods for wastewater decolorization. This process can be carried out with many methods, such as: biodegradation, coagulation/electrocoagulation, chemical oxidation or reverse osmosis. Sorption is believed to be one of the most economical and most safe to the environment method for color wastewater treatment.

Unlike precipitation methods, sorption does not increase wastewater salinity [5]; and unlike biological methods or

---

* Corresponding author.

in-depth oxidation, it does not result in the formation of toxic products of partial degradation of dyes [6]. The efficiency of wastewater decolorization via sorption depends mainly on the type of sorbent used, but also on the type of dyes and pH value. The costs of sorption are limited practically to the price of the sorbent. Commercial sorbents are quite expensive, which has prompted the search for cheaper but equally effective substitutes, which is why the popularity of unconventional sorbents is increasing. Today, the greatest hopes are fostered by sorbents acquisition from waste materials from the agri-food industry (plant biomass). Research on the sorption of pigments on such waste sorbents as: cereal biomass (wheat [7,8] and maize [9]), biomass of fruit plants (stems of pineapple [10], peels of bananas [11]) or breadnut peel [12], have already been reported. Sorptive abilities of coconut shells were examined as well [13]. A literature overview shows that the sorption capacity of the biomass-based sorbents is mainly due to the presence of cellulose, hemicellulose, and lignin [14], therefore the search for new biosorbents should be limited to the materials with a high content of polysaccharides and wood.

The high total content of polysaccharides and lignins (>85%) is typical of pumpkin seed husks (PSH) [15]. Pumpkin is a popular and widely available vegetable both in Europe and North America [16]. For these reasons, PSH are a potentially good raw material for the production of a sorbent efficient in dye sorption. In this study, the sorptive capabilities of *Cucurbita pepo* seed husks were tested against anionic dyes (Reactive Black 5, Reactive Yellow 84) and cationic dyes (Basic Violet 10, Basic Red 46) that are popular in the textile industry.

2. Materials

2.1. Pumpkin (Cucurbita pepo) seed husks

The PSH used in the study were obtained from fruit of a popular common pumpkin (*Cucurbita pepo*) variety Pepo produced by a Polish agricultural holding in the Orońsko commune in the Mazowieckie voivodeship. The chemical composition of seed husks of *C. pepo* var. Pepo used in the research is summarized in Table 1.

2.2. Dyes

Dyes used in the study were purchased from the BORUTA-ZACHEM SA dyes production plant in Zgierz

Table 1
Chemical composition of seed husks of pumpkin (*Cucurbita pepo* var. Pepo) [15]

Component	Content in dry matter [%]
Cellulose	39.9 ± 3.5
Hemicellulose	17.5 ± 1.0
Proteins	28.5 ± 1.2
Proteins, phytosterols, unsaturated fatty acids and others	≈14.5

(Poland). The specification of anionic dyes: Reactive Black 5 (RB5) and Reactive Yellow 84 (RY84); and of cationic dyes: Basic Violet 10 (BV10) and Basic Red 46 (BR46), provided by the manufacturer are presented in Table 2.

3. Methods

3.1. Sorbent preparation

PSH were ground in a laboratory mill and sifted through laboratory sieves with mesh diameters of 4 and 2 mm. The fraction with a diameter of 2–4 mm (free from particles of endosperm and flesh) was rinsed with distilled water and dried (4 h at 105°C). After drying, PSH were stored in an airtight container.

3.2. Determination of the influence of solution pH on the efficiency of dye sorption

PSH (PSH, 0.5 $g_{d.m.}$) were weighed into Erlenmeyer flasks (volume: 250 mL). Next, dye solutions (100 mL) with a concentration of 10 mg L^{-1} and with pHs of 2–11 were poured into the flasks and then the flasks were placed on a multi-station laboratory shaker SK-71 (150 r.p.m.) with a vibration amplitude of 3.0 cm (temp. 22°C). After 60 min of sorption, samples of the solutions (10 mL) were collected from the conical flasks to determine the concentration of the remaining dye.

3.3. Determination of the sorption equilibrium time

PSH (5.0 $g_{d.m.}$) were weighed into a series of beakers (volume: 1,000 mL). Next, dye solutions (1,000 mL, 10/50/100 mg L^{-1} – for RB5/RY84, 10/50/100/500 mg L^{-1} for BV10/BR46) with the optimal pH (established in point 3.2) were added to each beaker, after which the beakers were placed on a multi-station magnetic stirrer M5–53M (150 rpm, temp. 22°C). At defined intervals of time (after 0, 5, 10, 20, 30, 45, 60, 90, 120, 150, 180, and 240 min), samples of the solutions (5 mL) were collected from the beakers to determine the concentration of dye left in the solution.
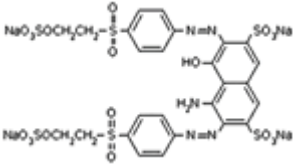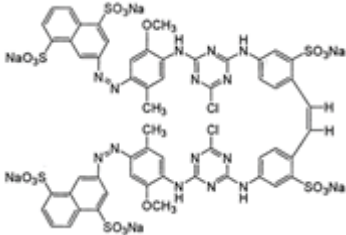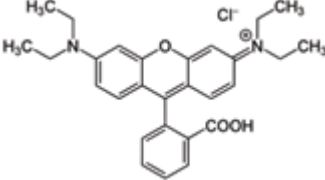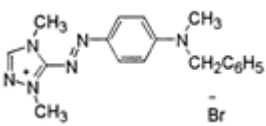
3.4. Determination of the maximum sorption capacity of PSH

PSH (0.5 $g_{d.m.}$) were weighed into a series of conical flasks (volume: 250 mL) and then dye solutions (100 mL) with the optimal pH (established in point 3.2) and concentrations in the range of 1–100 mg L^{-1} (for RB5/RY84) or 1–500 mg L^{-1} (for RB5/RY84) were added to the flasks. Then, the flasks were placed on a shaker (150 rpm) for the time needed to reach the sorption equilibrium (point 3.3), (temp. 22°C). Once the sorption reaction had been completed, a sample of the solution (10 mL) was collected from each flask to determine the concentration of dye left in the solution.

3.5. Fourier-transform infrared spectroscopy analysis of sorbent

The Fourier-transform infrared spectroscopy (FTIR) spectrum of PSH was achieved using the FT/IR-4700LE spectrometer (JASCO, Japan) with a single-reflection diamond ATR element. Sample scanning range covered infrared with a wavelength range of 4,000–600 cm⁻¹. The resolution of each

Table 2
Specification of RB5, RY84, BV10, and BR46 dyes

Reactive Black 5 - [RB5]		Reactive Yellow 84 - [RY84]	
Molar mass	991 (g mol⁻¹)	Molar mass	1,701 (g mol⁻¹)
Dye type	anionic	Dye type	anionic
λ_{max}	600 nm	λ_{max}	400 nm
Basic Violet 10 - [BV10]		Basic Red 46 - [BR46]	
Molar mass	479 (g mol⁻¹)	Molar mass	401 (g mol⁻¹)
Dye type	cationic	Dye type	cationic
λ_{max}	548 nm	λ_{max}	530 nm

spectrum was 1 cm⁻¹. The sample was measured 32 times and the results were averaged.

3.6. Calculation methods

The amount of dye adsorbed on PSH was calculated from Eq. (1):

$$Q_s = \frac{(C_0 - C_s) \cdot V}{m} \tag{1}$$

Studies on the dye sorption kinetics on PSH have been described using the pseudo-first-order (2) and pseudo-second-order (3) models, and also via the intramolecular diffusion model (4) (determination of the amount and intensity of sorption stages).

$$\frac{\Delta q}{\Delta t} = K_1 (q_e - q) \tag{2}$$

$$\frac{\Delta q}{\Delta t} = K_2 (q_e - q)^2 \tag{3}$$

$$q = k_{id} t^{0.5} \tag{4}$$

Langmuir 1 (Langmuir isotherm) (5), Langmuir 2 ("double" Langmuir isotherm), (6) and Freundlich model

(Freundlich isotherm) were used to determine the maximum sorption capacity (7).

The Langmuir isotherm equation (Eq. (2)):

$$Q_s = \frac{q_{max} \cdot K_c \cdot C}{1 + K_c \cdot C} \tag{5}$$

The Langmuir double isotherm equation (Eq. (3)):

$$Q_s = \frac{b_1 \cdot k_1 \cdot C}{1 + k_1 \cdot C} + \frac{b_2 \cdot k_2 \cdot C}{1 + k_2 \cdot C} \tag{6}$$

The Freundlich isotherm equation (Eq. (4)):

$$Q_s = K \cdot C^n \tag{7}$$

where Q_s – mass of absorbed dye (mg g⁻¹$_{d.m.}$); C_0 – initial concentration of dye (mg L⁻¹); C_s – concentration of dye after adsorption (mg L⁻¹); V – volume of dye (L); m – sorbent mass (PSH) (g$_{d.m.}$); q – momentary quantity of dye sorbed on PSH (mg g⁻¹$_{d.m.}$); k_{id} – adsorption rate constant in the intramolecular diffusion model (mg g⁻¹ min⁻⁰·⁵); t – time of sorption (min); q_e – equilibrium amount of dye absorbed on PSH (mg g⁻¹$_{d.m.}$); k_1 – sorption rate constant in the pseudo-first-order model (min⁻¹); k_2 – sorption rate constant in the pseudo-second order model (g mg⁻¹ min⁻¹); q_{max} – maximum sorption volume in the Langmuir 1 equation (mg g⁻¹$_{d.m.}$); K_c – constant in the Langmuir 1 equation (L mg⁻¹); C –

concentration of dye remaining in the solution (mg L^{-1}); b_1 – maximum sorption volume of sorbent (active sites of type I) (mg g$^{-1}_{d.m.}$); b_2 – maximum sorption volume of sorbent (active sites of type II) (mg g$^{-1}_{d.m.}$); k_1; k_2 – constants in the Langmuir 2 equation (L mg^{-1}); K – adsorption equilibrium constant in the Freundlich model; n – constant in the Freundlich equation; R^2 – coefficient of determination – a measure of data fit to the model; q_{exp} – experimental data – amount of adsorbed dye (mg g$^{-1}_{d.m.}$); q_{cal} – theoretical data resulting from the model – the amount of absorbed dye (mg g$^{-1}_{d.m.}$).

4. Results and discussion

4.1. FTIR analysis of PSH

The FTIR spectrum of PSH is shown in Fig. 1. The broad absorption band in the 3,000–3,700 cm^{-1} range shows the stretching of the O–H phenolic group of cellulose/hemicellulose and lignin. Peaks at 2,922 and 2,852 cm^{-1} show the

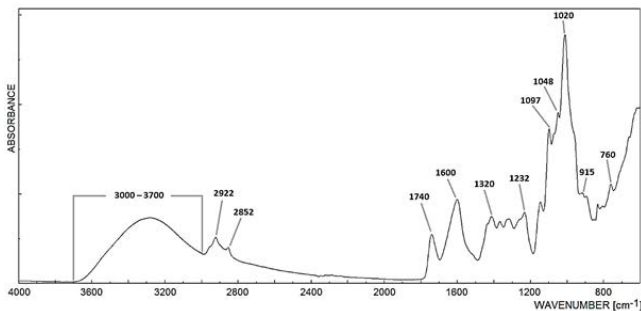Fig. 1. FTIR spectrum of pumpkin seeds husks.

C–H stretching of the aliphatic compounds. Clear peaks at 1,740 and 1,600 cm^{-1} indicate a C=O bond, typical of carbonyl groups of lignin or hemicellulose. Peaks at 1,320; 1,232; 1,097 and 1,048 cm^{-1} indicate the stretching of the C–O bond. A very pronounced peak at 1,020 cm^{-1} (stretching of C–O–C bonds) indicates the presence of saccharide structures in the material. The presence of glycosidic polysaccharide bonds is indicated by peaks at 915 and 760 cm^{-1}.

4.2. Effect of solution pH on dyes sorption on PSH

In the initial pH range of 2–11, the sorption efficiency of anionic dyes (RB5 and RY84) on PSH decreased along with increasing initial pH of the solution. In the case of both RB5 and RY84, the highest decolorization rate of the solution was determined at the initial pH 2, and the lowest one at pH 11. The greatest decrease in the binding efficiency of RB5 and RY84 to PSH was noted in the pH range of 2–3 (Figs. 2a and b).

At low pH, hydroxyl functional groups of the polysaccharides present in the PSH structure, such as cellulose or hemicellulose, can be protonated according to the reaction: R-CH$_2$-OH + H$_3$O$^+$ → R-CH$_2$-OH$_2^+$ + H$_2$O. The protonated hydroxyl group may additionally separate from the polysaccharide chain in the form of a water molecule according to the reaction: R-CH$_2$-OH$_2^+$ → R-CH$_2^+$ + H$_2$O, however this process takes place much slower than the protonation of the hydroxyl group. In both cases, the polysaccharides finally gain a positive charge. The number of the displaced hydroxyl groups and the total positive charge on the surface of the sorbent increase as solution pH decreases. The positively charged hydroxyl groups present in PSH attract electrostatically the molecules of anionic
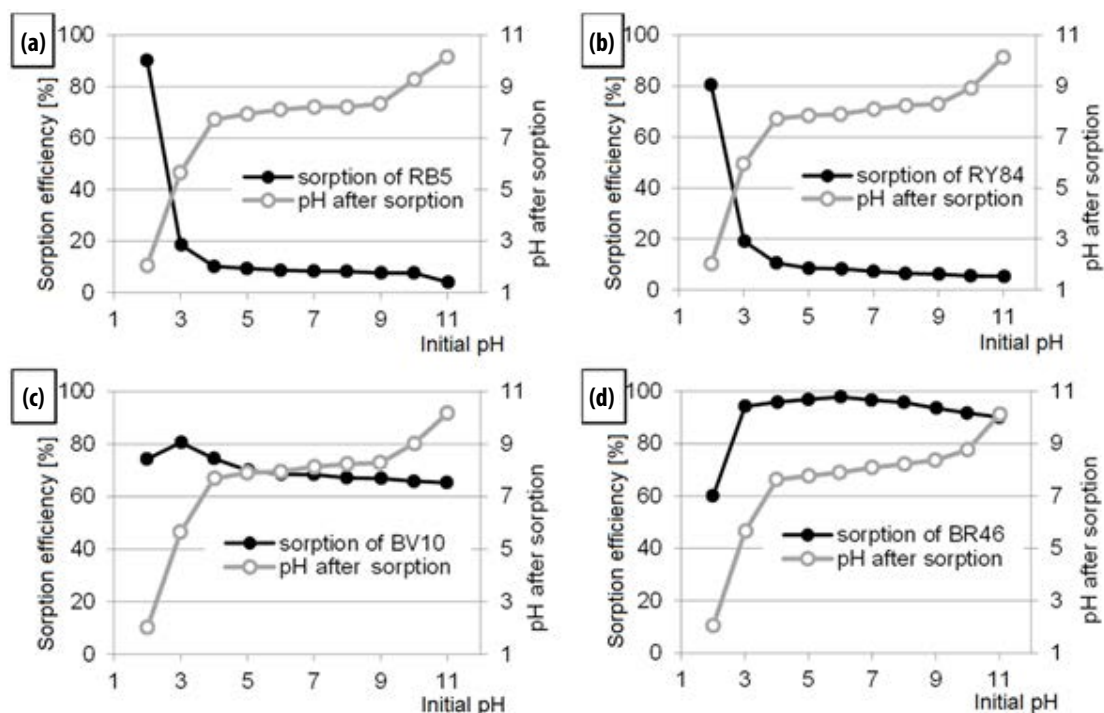

Fig. 2. Effect of solution pH on the efficiency of dye sorption on PSH. (a) RB5, (b) RY84, (c) BV10 and (d) BR46.

dyes, which greatly support their sorption. The electrostatic attraction force of dyes depends on the number of proton functional groups, which explains the increase in the sorption efficiency of RB5 and RY84 along with a decreasing pH value. Hydroxyl functional hydrocarbon groups occurring in the PSH structure are easily protonated at very low pH (pH < 3). This explains the very large decrease in the sorption efficiency of RB5 and RY84 in the pH range of 2–3, as well as the low binding efficiency of RB5 and RY84 to PSH in the pH range of 4–10. Deprotonation of hydroxyl functional groups of polysaccharides is likely at very high pH values, owing to which PSH can gain a negative charge. The negatively charged surface of the sorbent can electrostatically repel anionic dyes, which can additionally impede their sorption. Therefore, the sorption of RB5 and RY84 on PSH was the least effective at pH 11 (Figs. 2a and b). A similar effect of solution pH on the sorption efficiency was noted in studies on the sorption of anionic dyes on banana peel [17], rice bran [18], and coconut shell [19].

The sorption efficiency of the cationic dye BV10 on PSH was the highest at pH 3 and decreased with solution pH increase from 3 to 11 (Fig. 2c). Despite the decrease in the sorption efficiency along with an increasing initial pH, BV10 removal in the pH range of 5–11 sustained at a relatively high level.

A characteristic feature of BV10 is its carboxylic functional group (–COOH) capable of generating a local negative charge. The negatively charged carboxyl group of BV10 (–COO⁻) interacted electrostatically with the positively charged PSH surface at low pH (pH 2–4), which explains the high sorption efficiency of the cationic dye at pH 3. At pH < 3, most of the BV10 carboxylic groups are in the undissociated form (–COOH), while the majority of xanthene groups are in the protonated form (pKa for BV10 = 3.1) [20]. A low number of deprotonated carboxylic groups (–COO⁻) translates into a weaker interaction with the positively charged surface of the sorbent, which explains the lower sorption of the dye at pH 2 compared to pH 3. A slight decrease in the sorption efficiency of BV10 at pH 2 may also result from dye competition with chloride ions (Cl⁻) for PSH sorption centers. A similar effect of solution pH on the efficiency of BV10 sorption was noted in studies with pine

bark [21] and shrimp shells [22] used for the decolorization of aqueous solutions.

The sorption of cationic dye BR46 on PSH was effective over a wide range of pH values, that is, pH 3–8, however, the highest binding efficiency was observed at pH 6 (Fig. 2d). The high efficiency of sorption in a wide pH range is a phenomenon typical of the sorption of alkaline dyes [23,24]. A characteristic feature of BR46 solutions is their decolorization at pH > 8, therefore the results of BR46 sorption on PSH at pH 9–11 have not been included in the graph (Fig. 2d).

At pH 2, the positively charged PSH surface as a result of the displacement of the functional groups, repelled electrostatically the particles of the cationic dye during sorption. This explains the low efficiency of BR46 binding to PSH at pH < 3. Similar results were obtained in the research concerning BR46 sorption on charcoal originating from the milk vetch [25], pine leaves [26], and charcoal from wild olive wood [27].

PSH influenced the pH change of the solutions during sorption (Fig. 3). Systems with dye solutions sought to achieve a pH close to the pH_{PZC} value of the sorbent, which is a typical phenomenon during sorption under static conditions. The experimentally determined zero charge point value for PSH was $pH_{PZC} \sim 8.00$ (Fig. 3).

Due to the fact that the process of fabrics dyeing with anionic dyes usually takes place at pH 3.5–7.0 [17], the pH of color wastewater seldom reaches values below pH 3. Therefore, although the sorption of RB5 and RY84 was the most efficient at pH 2, further experiments on the sorption of anionic dyes were carried out at the initial pH of 3. In the case of the cationic dyes, the optimal pH of sorption (pH 3 for BV10 and pH 6 for BR46) was used in the next stages of analyses.

4.3. Kinetics of dyes sorption on PSH

The time needed to reach sorption equilibrium for RB5 and RY84 dyes on PSH was independent of the initial dye concentration and ranged from 150 to 180 min (Figs. 4a and b). A similar time of reaching sorption equilibrium was also obtained in studies addressing RB5 sorption on wheat straw (195 min) [28], shells of sunflower seeds (210 min) [29], and commercial activated carbon (180 min) [30].
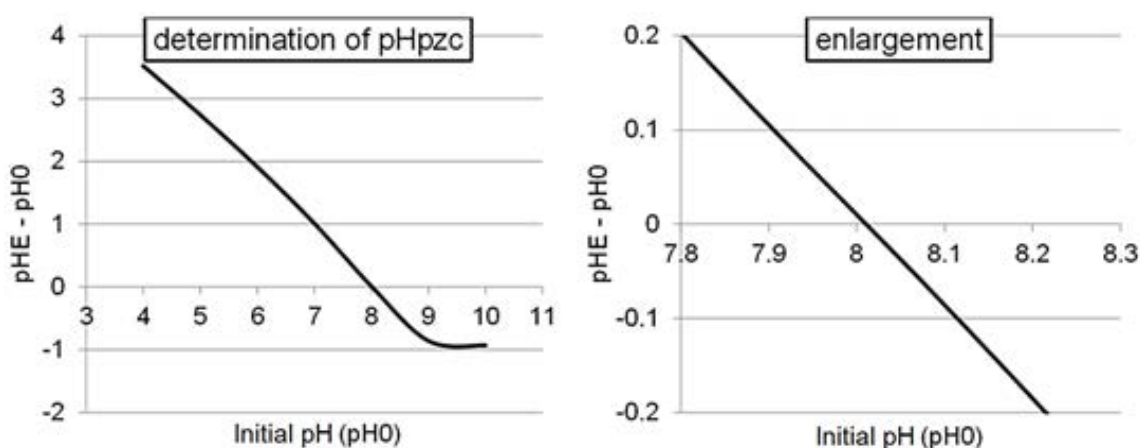

Fig. 3. Determination of pH_{PZC} for PSH.

Time required achieving the sorption equilibrium for the cationic dye BV10 was similar to that of anionic dyes RB5 and RY84 and reached 180 min irrespective of the initial dye concentration (Fig. 4c). A similar observation was made for the sorption of cationic dyes on oak acorns [31] or sugar cane [32].

The sorption equilibrium time for BR46 was dependent on initial dye concentration of the dye and reached 60, 90, 90, and 180 min at dye concentrations of 10, 50, 100, and 500 mg L^{-1}, respectively. The shorter sorption time of BR46 on PSH at its lower initial concentrations resulted from the rapid depletion of available dye molecules, which prevented their further sorption (Fig. 4d). In the system enabling the complete saturation of PSH sorption centers (500 mg RB46/L concentration), the equilibrium time of sorption was similar to that of other dyes (180 min).

Regardless of the chemical character and initial concentration of the dye, the kinetics of its sorption on PSH was best described by the pseudo-second-order model (Table 3). The sorption capacities calculated from this model ($q_{e,cal}$) increased for each dye as their initial concentration increased, which in the systems ensuring saturation of sorption centers (number of dye molecules > number of free active sites) may indicate a relatively low affinity of the sorbate for the sorbent. In each experimental series, the value of the reaction rate constant k_2 decreased with the increase of the initial dye concentration, which is typical of the sorption of dyes on activated carbon from biomass [33,34].

The model of intramolecular diffusion adapted to the experimental data indicated that the sorption of the tested dyes on PSH took place in three main stages (Table 4). At the first stage, the shortest but the most intense one, diffusion of dye molecules from the solution to the surface of the sorbent occurred and most of the available sorption centers were occupied. Despite its short duration, the amount of dye bound at this stage ranged from 41% to 66% of the q_e value (the amount of dye bound after the equilibrium time). At the second stage, easily accessible sites on the PSH surface were exhausted and competition between dye molecules was growing, which resulted in sorption process slowdown and its efficiency decrease. At the third, the longest and the least intensive stage, the last free sorption centers were probably located in deeper, harder to reach layers of the sorbent.

Regardless of dye type and initial concentration, the first stage lasted 10 min. However, the initial concentration of dye had a great impact on the duration of the second stage, which shortened as dye concentration increased. It was related to the increasing rate of the saturation of sorption centers and a faster transition of the process to the last stage. This tendency was not observed for BR46 dye due to the binding of most dye molecules already at the first sorption stage (10–100 mg L^{-1} concentration). Intermolecular diffusion rate constants (k_{d1}, k_{d2}, k_{d3}) indicate that in each of the three stages, the intensity of the process increased with the initial concentration of the dye in the solution. This can be explained by the higher probability of dye molecules colliding with sorption centers at their higher concentration in the solution.

The sorption of anionic dyes RB5 and RY84 on PSH was significantly less efficient than the sorption of cationic dyes (BV10 and BR46) (Tables 3 and 4). This could probably be due to a very small amount of base functional groups on PSH surface (easily protonated with pH < pH$_{PZC}$), being the main sorption centers for anionic dyes. Because of the high content of cellulose and hemicellulose in PSH, most of the groups on its surface were the hydroxyl groups. At pH 3 which was used in the experiment, only a few of these groups were protonated ($-OH + H_3O^+ \rightarrow -OH_2^+ + H_2O$), which resulted in poor electrostatic interaction with dye anions.
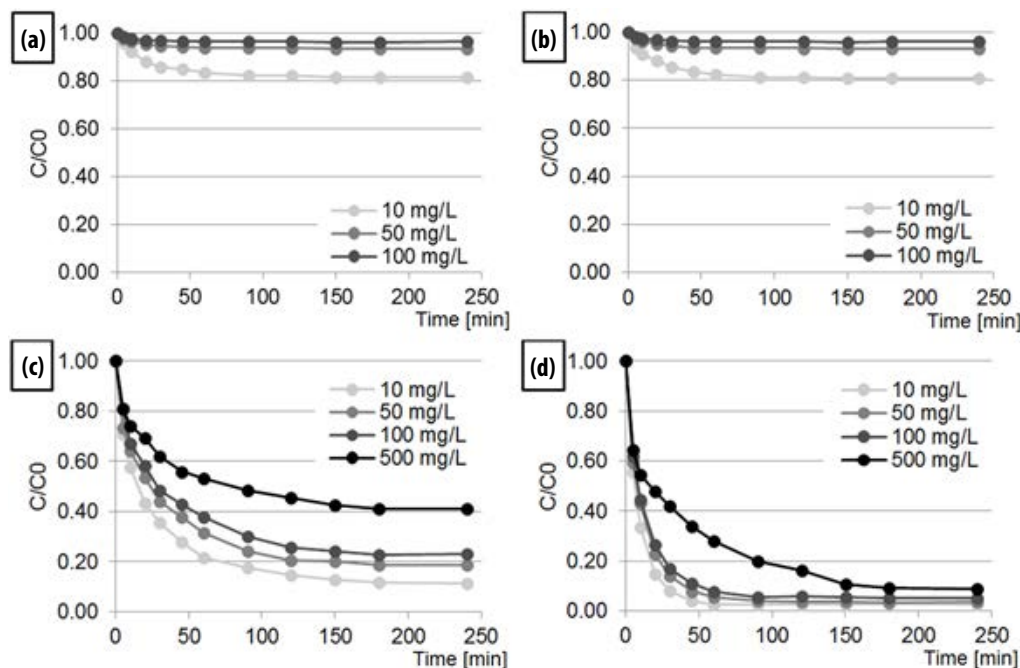

Fig. 4. Changes in dye concentrations during sorption on PSH. (a) RB5, (b) RY84, (c) BV10 and (d) BR46

Table 3
Kinetic parameters of dye sorption on PSH from the pseudo-first and pseudo-second-order models

Dye	Concentration of dye (mg L^{-1})	Pseudo-first-order model			Pseudo-second-order model			Exper. data
		$q_{e,cal}$	K_1	R^2	$q_{e,cal}$	K_2	R^2	$q_{e,exp}$
		(mg g^{-1})	(min^{-1})	-	(mg g^{-1})	(g mg^{-1} min^{-1})	-	(mg g^{-1})
RB5	10	0.36	0.051	0.9933	0.40	0.168	0.9955	0.37
	50	0.65	0.076	0.9878	0.69	0.162	0.9973	0.65
	100	0.73	0.105	0.9885	0.78	0.157	0.9972	0.75
RY84	10	0.38	0.057	0.9846	0.41	0.197	0.9950	0.38
	50	0.67	0.080	0.9826	0.73	0.164	0.9964	0.69
	100	0.80	0.105	0.9912	0.86	0.192	0.9962	0.82
BV10	10	1.69	0.057	0.9760	1.87	0.043	0.9986	1.77
	50	7.82	0.047	0.9665	8.73	0.007	0.9926	8.13
	100	14.83	0.041	0.9739	16.79	0.003	0.9952	15.39
	500	55.53	0.043	0.9517	62.41	0.001	0.9860	59.03
BR46	10	1.94	0.115	0.9987	2.06	0.090	0.9987	1.95
	50	9.52	0.092	0.9941	10.25	0.014	0.9936	9.62
	100	18.66	0.087	0.9934	20.16	0.007	0.9952	18.96
	500	84.08	0.051	0.9071	92.92	0.001	0.9663	91.08

Table 4
Constant rates of intramolecular diffusion of dyes determined from a simplified model of intramolecular diffusion. Units: k_{d1}, k_{d2}, k_{d3} = (mg g^{-1} min$^{-0.5}$)

Dye	Conc. of dye (mg L^{-1})	First stage of sorption			Second stage of sorption sorption			Third stage of sorption sorption		
		k_{d1}	Time (min)	R^2	k_{d2}	Time (min)	R^2	k_{d2}	Time (min)	R^2
RB5	10	0.047	~10	0.9817	0.030	~80	0.8964	0.004	~90	0.8903
	50	0.114	~10	0.9977	0.056	~50	0.9654	0.005	~90	0.7708
	100	0.156	~10	0.9971	0.059	~35	0.9753	0.007	~105	0.9336
RY84	10	0.058	~10	0.9999	0.031	~80	0.9343	0.002	~60	0.9808
	50	0.125	~10	0.9995	0.071	~35	0.9943	0.008	~150	0.9741
	100	0.164	~10	0.9998	0.098	~20	0.9963	0.009	~150	0.8690
BV10	10	0.266	~10	0.9996	0.126	~80	0.9750	0.031	~90	0.9784
	50	1.143	~10	0.9986	0.631	~80	0.9389	0.135	~90	0.9004
	100	2.013	~10	0.9826	1.299	~50	0.9807	0.522	~120	0.9223
	500	8.214	~10	0.9995	5.275	~35	0.9877	2.250	~135	0.9922
BR46	10	0.415	~10	0.9982	0.226	~20	0.9651	0.049	~30	0.9679
	50	1.800	~10	0.9999	1.281	~20	0.9801	0.234	~60	0.8455
	100	3.484	~10	0.9996	2.420	~20	0.9900	0.550	~60	0.9021
	500	16.621	~10	0.9934	5.639	~80	0.9967	2.876	~90	0.9712

The sorption of cationic dyes on PSH was effective, inter alia, due to the high content of nitrogen in the dye molecules and the possibility of generating a large number of hydrogen bonds with hydroxyl groups of the sorbent. Because of to the high content of nitrogen in the molecules, BR46 and BV10 could efficiently bind to PSH by creating hydrogen bridges with hydroxyl groups of polysaccharides (–RN~HO–R). As a result, sorption of BR46 and BV10 on PSH could be effective even with a minimal effect of electrostatic interaction with the sorbent's surface.

4.4. Sorption capacity of PSH

Fig. 5 shows the experimental data described by Langmuir 1, Langmuir 2, and Freundlich sorption isotherms. For each dye, Lamgmuir's double isotherm showed the greatest fit to the experimental data obtained (Table 5).

Better fit of the Langmuir 2 model to the experimental data in comparison with the Langmuir 1 model most probably indicates the presence of at least 2 types of sorption centers. Polysaccharides present in PSH (cellulose,
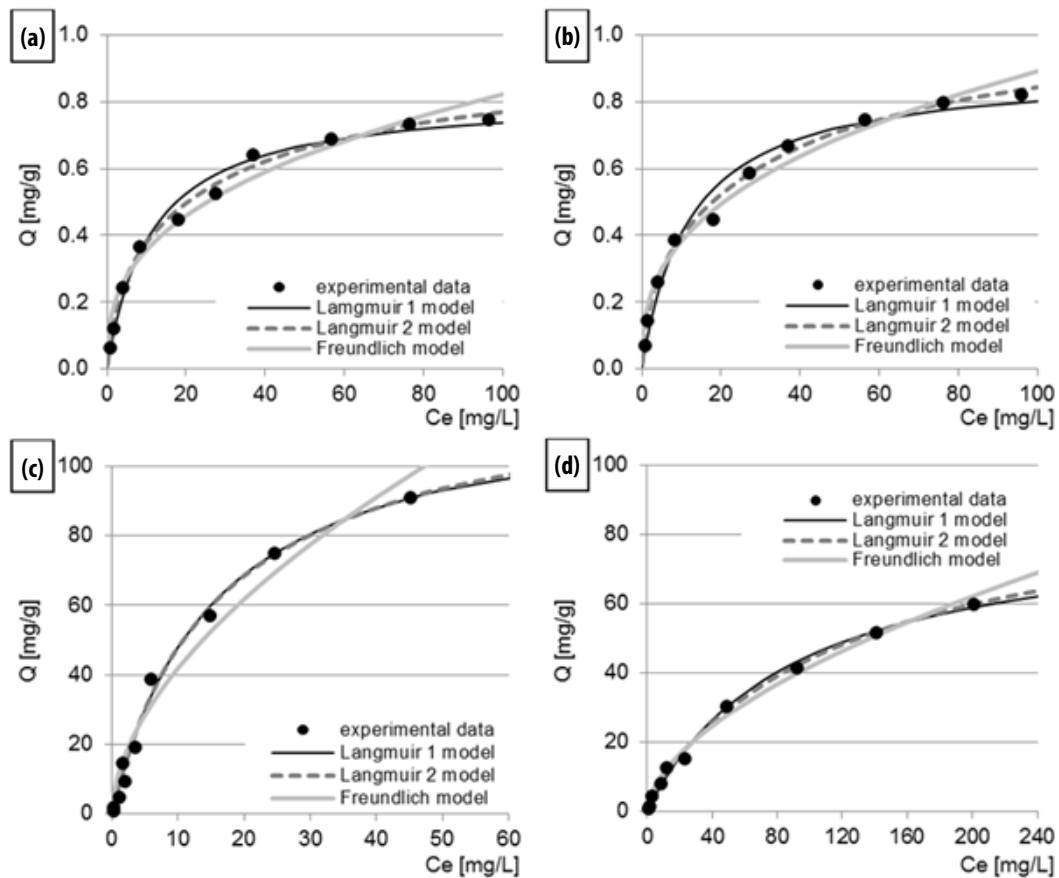
Fig. 5. Isotherms of the sorption of dyes: (a) RB5, (b) RY84, (c) BV10 and (d) BR46 on PSH. Langmuir 1, Langmuir 2, and Freundlich isotherms.

Table 5
Constants determined from Langmuir 1, Langmuir 2 and Freundlich isotherms

Model (isotherm)	Constants in sorption model	RB5	RY84	BV10	BR46
	q_{max} (mg $g^{-1}_{d.m.}$)	0.82	0.90	85.07	121.71
Langmuir 1	K_c (L $g^{-1}_{d.m.}$)	0.089	0.083	0.011	0.065
	R^2	0.983	0.974	0.992	0.992
	q_{max} (mg $g^{-1}_{d.m.}$)	0.96	1.08	96.01	163.39
	b_1 (mg $g^{-1}_{d.m.}$)	0.64	0.79	91.36	113.77
	b_2 (mg $g^{-1}_{d.m.}$)	0.32	0.29	4.65	49.62
Langmuir 2	k_1 (L mg^{-1})	0.026	0.024	0.008	0.070
	k_2 (L mg^{-1})	0.354	0.538	0.306	0.002
	R^2	0.994	0.993	0.997	0.995
	K (–)	0.155	0.164	11.525	2.967
Freundlich	n (L $g^{-1}_{d.m.}$)	0.363	0.367	0.560	0.574
	R^2	0.968	0.977	0.970	0.992

hemicellulose) contain mainly hydroxyl groups. For this reason, the various active sites of PSH are presumably only –OH groups but having a different degree of affinity to the sorbate (k_1/k_2). Different degrees of hydroxyl group affinity to dyes may result from different methods of their binding to the dye (physical adsorption/chemisorption) or from different

location of –OH groups (easily accessible surface and deeper sorbent layers are difficult to access).

The maximum sorption capacity of PSH against the anionic dyes was low and amounted to 0.96 mg g^{-1} for RB5 and to 1.08 mg g^{-1} for RY84 (Table 5). Constants b_1, b_2, k_1, k_2 determined from the Langmuir 2 model for RB5 and RY84

Table 6
Summary of sorption capacities of various sorbents against dyes tested: RB5, RY84, BV10, and BR46 (literature data)

Dye (chemical character of the dye)	Type of sorbent used	Sorption capacity (mg g^{-1}$_{d.m.}$)	pH of sorption	Time of sorption (min)	Sources
RB5 (anionic)	Pumpkin seed husks	1.0	3	60	This study
	Sunflower seeds husks	1.1	3,5	120	[29]
	Straw from wheat	15.7	7	205	[8]
	Active carbon from nut wood	19.3	5	402	[37]
RY84 (anionic)	Pumpkin seed husks	1.1	3	60	This study
	Compost	2.2	3	180	[38]
	Wool	7.0	11	180	[39]
	Bone meal	57.2	6,6	120	[40]
BV10 (cationic)	Orange peels	3.2	4	b.d.	[35]
	Banana peels	20.6	6	1440	[35]
	Baker's yeast	25.2	6.5	72	[41]
	Active carbon from palm bark	30.00	3	b.d.	[42]
	Pumpkin seed husks	96.0	3	60	This study
BR46 (cationic)	Sawdust fir	20.5	b.d.	120	[43]
	Active carbon from biomass	65.7	7	90	[36]
	Coconut shells	68.5	6	120	[13]
	Pumpkin seed husks	163.4	6	60	This study

had similar values, which may indicate a similar sorption mechanism. Presumably, the anionic dyes tested were not able to attach to sorptive centers located in the deeper layers of PSH due to their high molar mass and acidity. Presumably, some of the dyes were combined with PSH hydroxyl groups on the basis of electrostatic interaction (physical adsorption) (b_1, k_1), and some joined permanently with –OH groups on the basis of chemisorption (b_2, k_2).

The PSH sorption capacity obtained for the cationic dyes was much higher than for the anionic ones. The maximum sorption capacity of pumpkin seeds husks calculated from the Langmuir 2 model was 96.01 mg g^{-1} for BV10 and 163.39 mg g^{-1} for BR46 (Table 3). Differences in the degree of affinity of cationic dyes to the sorption centers (k_1 and k_2) probably arise from different locations of PSH hydroxyl functional groups. As mentioned in section 4.3, the lower sorption efficiency of the anionic dyes on PSH compared to the cationic dyes was presumably due to the low susceptibility of hydroxyl functional groups to protonation at pH 3, which translated into weaker electrostatic interaction of RB5 and RY84 with PSH. The advantage of the tested cationic dyes (BV10, BR46) over anionic dyes was also the possibility of producing more hydrogen bonds with hydroxyl groups of PSH, owing to which the dye could effectively bind to the sorbent even at suboptimal pH.

Table 6 compares sorption capacities of various sorbents (literature data) with that of PSH tested in this study against RB5, RY84, BV10, and BR46 dyes. Unmodified lignocellulosic sorbents, such as seed husks or plant biomass, have a low sorption capacity against anionic dyes (Table 6). For this reason, they are not recommended as sorbents for the decolorization of wastewater containing acidic or reactive dyes. However, PSH tested in our study shows very high efficiency in relation to cationic dyes. With respect to the BV10 and BR46 dyes tested, the PSH had a higher sorption capacity than other unconventional lignocellulosic sorbents, such as fruit peel [35] or coconut shells [13]. PSH had even a higher sorption capacity against BR46 compared to the activated carbon produced from plant biomass [36].

5. Conclusions

Properly prepared PSH can be an effective sorbent for cationic dyes. The efficiency of dye sorption on PSH depended on the chemical character of the dye. Due to the low number of base functional groups in the sorbent's structure, the sorption efficiency of the anionic dyes (Q_{max} = 0.96 mg RB5 g^{-1}, 1.08 mg RY84 g^{-1}) was low compared to that of the cationic dyes (Q_{max} = 96.01 mg BV10 g^{-1}, 163.39 mg BR46 g^{-1}). A significant advantage of BV10 and BR46 over RB5 and RY84 was their potential to produce more hydrogen bonds with the polysaccharides present in PSH (N~H).

The efficiency of dye sorption on PSH largely depended on solution pH. The optimal pH range for the sorption of anionic dyes on PSH was pH 2–3. The sorption of the BV10 cationic dye on PSH occurred most effectively at pH 3, while the sorption efficiency of BR46 on the sorbent tested was the highest at pH 6.

The time needed to reach dye sorption equilibrium on PSH was similar to that of the other sorbents based on lignocellulosic materials and ranged from 150 to 180 min regardless of the initial concentration of dye.

Dye sorption on PSH proceeded in three main stages, varying in intensity and duration. The amount of dye bound in stage 1, despite its short duration (~10 min), ranged from 41% to 66% of the q_e value.

PSH have at least 2 types of active sites. The various PSH active sites are presumably hydroxy groups having a

different degree of affinity to the sorbate. It may result from different location of the –OH groups (easily accessible surface and harder deeper layers of the sorbent).

Acknowledgements

References

[1] A. Paz, J. Carballo, M.J. Perez, J.M. Dominguez, Biological treatment of model dyes and textile wastewaters, Chemosphere, 181 (2017) 168–177.
[2] K. Meerbergen, S. Crauwels, K.A. Willems, R. Dewil, J. Van Impe, L. Appels, B. Lievens, Decolorization of reactive azo dyes using a sequential chemical and activated sludge treatment, J. Biosci. Bioeng., 124 (2017) 668–673.
[3] C.C. Hsueh, C.T. Chen, A.W. Hsu, C.C. Wu, B.Y. Chen, Comparative assessment of azo dyes and nitroaromatic compounds reduction using indigenous dye-decolorizing bacteria, J. Taiwan Inst. Chem. Eng., 79 (2017) 134–140.
[4] M. Solis, A. Solis, H.I. Perez, N. Manjarrez, M. Flores, Microbial decolouration of azo dyes: a review, Process Biochem., 47 (2012) 1723–1748.
[5] Y. Wei, Q. Ji, L. Chen, J. Hao, Ch. Yao, X. Dong, Preparation of an inorganic coagulant-polysilicate-magnesium for dyeing wastewater treatment: effect of acid medium on the characterization and coagulation performance, J. Taiwan Inst. Chem. Eng., 72 (2017) 142–148.
[6] A. Anielak, Chemiczne i fizykochemiczne oczyszczanie ścieków (Chemical and physicochemical wastewater treatment), Wydawnictwo Naukowe PWN, Warszawa (Scientific Publisher PWN, Warsaw), 2000, pp. 292–297.
[7] U. Farooq, J.A. Kozinski, M.A. Khan, M. Athar, Biosorption of heavy metal ionic using wheat based biosorbents-A review of the recent literature, Bioresour. Technol., 101 (2010) 5043–5053.
[8] W. Zhang, H. Yan, H. Li, Z. Jiang, L. Dong, X. Kan, H. Yang, A. Li, R. Cheng, Removal of dye from aqueous solutions by straw based adsorbents: batch and column studies, Chem. Eng. J., 168 (2011) 1120–1127.
[9] E.J. Lara-Vasquez, M. Solache-Rios, E. Gutierrez-Segura, Malachite green dye behaviours in the presence of biosorbents from maize (*Zea mays* L.), their Fe-Cu nanoparticles composites and Fe-Cu nanoparticles, J. Environ. Chem. Eng., 4 (2016) 1594–1603.
[10] S.L. Chan, Y.P. Tan, A.H. Abdullah, S.T. Ong, Equilibrium, kinetic and thermodynamic studies of a new potential biosorbent for the removal of Basic Blue 3 and Congo Red dyes: Pineapple (*Ananas comosus*) plant stem, J. Taiwan Inst. Chem. Eng., 61 (2016) 306–315.
[11] T. Ahmad, M. Danish, Prospects of banana waste utilization in wastewater treatment: a review, J. Environ. Manage., 206 (2018) 330–348.
[12] L.B.L. Lim, N. Priyantha, D.T.B. Tennakoon, H.I. Cheing, M.K. Dahri, M. Suklueng, Breadnut peel as a highly effective low-cost biosorbent for methylene blue: equilibrium, thermodynamic and kinetic studies, Arabian J. Chem., 10 (2017) 3216–3228.
[13] A. Bhatnagar, V.J.P. Vilar, C.M.S. Botelho, R.A.R. Baaventura, Coconut-based biosorbents for water treatment: a review of the recent literature, Adv. Colloid Interface Sci., 160 (2010) 1–15.
[14] D.P. Dutta, S. Nath, Low cost synthesis of SiO_2/C nanocomposite from corn cobs and its adsorption of uranium (VI), chromium (VI) and cationic dyes from wastewater, J. Mol. Liq., 269 (2018) 140–151.
[15] F.S. Calixto, J. Canellas, J.G. Raso, Determination of hemicellulose, cellulose and lignin contents of dietary fibre and crude fibre of several seed hulls. Data comparison, Z. Lebensm. Unters. Forsch., 177 (1983) 200–202.

[16] P. Schinas, G. Karavalakis, C. Davaris, G. Anastopoulos, D. Karonis, F. Zannikos, S. Stournas, E. Lois, Pumpkin (*Cucurbita pepo* L.) seed oil as an alternative feedstock for the production of biodiesel in Greece, Biomass Bioenergy, 33 (2009) 44–49.
[17] V. Subbaiah Munagapati, V. Yarramuthi, K.M. Lee, D.-S. Kim, Removal of anionic dyes (Reactive Black 5 and Congo Red) from aqueous solutions using banana peel powder as an adsorbent, Ecotoxicol. Environ. Saf., 148 (2018) 601–607.
[18] F. Ogata, D. Imai, N. Kawasaki, Cationic dye removal from aqueous solution by waste biomass produced from calcination treatments of rice bran, J. Environ. Chem. Eng., 3 (2015) 1476–1485.
[19] T. Jóźwiak, U. Filipkowska, P. Bugajska, T. Kalkowski, The use of coconut shells for the removal of dyes from aqueous solution, J. Ecol. Eng., 19 (2018) 129–135.
[20] K. Shena, M.A. Gondal, Removal of hazardous Rhodamine dye from water by adsorption onto exhausted coffee ground, J. Saudi Chem. Soc., 21 (2017) 120–127
[21] R. Ahmad, Studies on adsorption of crystal violet dye from aqueous solution onto coniferous pinus bark powder (CPBP), J. Hazard. Mater., 171 (2009) 767–773.
[22] S. Gopi, A. Pius, S. Thomas, Enhanced adsorption of crystal violet by synthesized and characterized chitin nano whiskers from shrimp shell, J. Water Process Eng., 14 (2016) 1–8.
[23] I. Homelnicu, A. Baiceanu, M.-E. Ignat, V. Dulman, The removal of Basic Blue 41 textile dye from aqueous solution by adsorption onto natural zeolitic tuff: kinetics and thermodynamics, Process Saf. Environ., 105 (2017) 274–287.
[24] M.A.M. Salleh, D.K. Mahmoud, W.A.W.A. Karim, A. Idris, Cationic and anionic dye adsorption by agricultural solid wastes: a comprehensive revive, Desalination, 280 (2011) 1–13.
[25] S. Jorfi, R.D.C. Soltani, M. Ahmadi, A. Khataee, M. Safari, Sono-assisted adsorption of a textile dye on milk vetch-derived charcoal supported by silica nanopowder, J. Environ. Manage., 187 (2017) 111–121.
[26] F. Deniz, S. Karaman, Removal of Basic Red 46 dye from aqueous solution by pine tree leaves, Chem. Eng. J., 170 (2011) 67–74.
[27] F. Kaouah, S. Boumaza, T. Berrama, M. Trari, Z. Bendjama, Preparation and characterization of activated carbon from wild olive cores (oleaster) by H_3PO_4 for removal of Basic Red 46, J. Cleaner Prod., 1 (2013) 296–306.
[28] N. Yousefi, A. Fatehizadeh, E. Azizi, M. Ahmadian, A. Ahmadi, A. Rajabizadeh, A. Toolabi, Adsorption of reactive black 5 dye onto modified wheat straw: isotherm and kinetics study, Sacha J. Environ. Stud., 1 (2011) 81–91.
[29] J.F. Osma, V. Saravia, J.L. Toca-Herrera, S.C. Couto, Sunflower seed shells: a novel and effective low-cost adsorbent for the removal of the diazo dye Reactive Black 5 from aqueous solutions, J. Hazard. Mater., 147 (2007) 900–905.
[30] M.C. Ribas, M.A. Adebayo, L.D.T. Prola, E.C. Lima, R. Cataluñab, L.A. Feris, M.J. Puchana-Rosero, F.M. Machado, F.A. Pavan, T. Calvete, Comparison of a homemade cocoa shell activated carbon with commercial activated carbon for the removal of reactive violet 5 dye from aqueous solutions, Chem. Eng. J., 248 (2014) 315–326.
[31] S. Kuppusamy, K. Venkateswarlu, P. Thavamani, Y.B. Lee, R. Naidu, M. Megharaj, Quercus robour acorn peel as a novel coagulating adsorbent for cationic dyes removal from aquatic ecosystems, Ecol. Eng., 101 (2017) 3–8.
[32] J.X. Yu, J. Zhu, L.Y. Feng, R.A. Chi, Simultaneous removal of cationic and anionic dyes by the mixed sorbent of magnetic and non-magnetic modified sugarane bagasse, J. Colloid Interface Sci., 458 (2015) 153–160.
[33] M.A. Ahmad, N.A.A. Puad, O.S. Bello, Kinetic, equilibrium and thermodynamic studies of synthetic dye removal using pomegranate peel activated carbon prepared by microwave-induced KOH activation, Water Res. Ind., 6 (2014) 18–35.
[34] T. Santhi, S. Manonmani, T. Smitha, Kinetics and isotherm studies on cationic dyes adsorption onto annona squmosa seed activated carbon, Int. J. Eng. Sci. Technol., 2 (2010) 287–295.
[35] C. Namasivayam, N. Kanchana, R.T. Yamuna, Waste banana pith as adsorbent for the removal of rhodamine-B from aqueous solutions, Waste Manage., 13 (1993) 89–95.

[36] N.A.I. Azmi, N.F. Zainudin, U.F.M. Ali, F. Senusi, Adsorption kinetics on Basic Red 46 removal using *Cerbera odollam* activated carbon, J. Eng. Sci. Technol., 3 (2015) 82–91.

[37] Heibati, S. Rodriguez-Couto, A. Amrane, M. Rafatullah, A. Hawari, M.A. Al-Ghouti, Uptake of Reactive Black 5 by pumice and walnut activated carbon: chemistry and adsorption mechanisms, J. Ind. Eng. Chem., 20 (2014) 2939–2947.

[38] T. Jóźwiak, U. Filipkowska, J. Rodziewicz, A. Mielcarek, D. Owczarkowska, Application of compost as a cheap sorbent for dyes removal from aqueous solutions, Rocz. Ochr. Sr., 15 (2013) 2398–2411.

[39] E. Sahin, Interpretation of sorption kinetics for mixtures of reactive dyes on wool, Turk. J. Chem., 29 (2010) 617–625.

[40] M. Arshadi, A.R. Faraji, M.J. Amiri, M. Mehravar, A. Gil, Removal of methyl orange on modified ostrich bone waste - a novel organic – inorganic biocoposite, J. Colloid Interface Sci., 446 (2015) 11–23.

[41] M.S. Mahmoud, Decolorization of certain reactive dye from aqueous solutions using Baker's Yeast (*Saccharomyces cerevisiae*) strain, HBRC J., 12 (2016) 88–98.

[42] M. Mohammadi, A.J. Hassani, A.R. Mohamed, G.D. Najafpour, Removal of Rhodamine B from aqueous solution using palm shell-based activated carbon, adsorption and kinetic studies, J. Chem. Eng. Data, 55 (2010) 5777–5785.

[43] A. Shukla, Y.-H. Zhang, P. Dubey, J.L. Margrave, S.S. Shukla, The role of sawdust in the removal of unwanted materials water, J. Hazard. Mater., 95 (2002) 137–152.